SMiRT-12 / K. Kussmaul (Editor)

E01/5

EXPERIMENTAL TESTS AND NUMERICAL CALCULATIONS OF REINFORCED CONCRETE SLABS SUBJECTED TO RIGID MISSILE IMPACT

F. Corsi[1], P. Di Giamberardino[1], H. Bung[2], M. Lepareux[2] and Ph. Matheron[2]

[1]ENEA C.R.E. Casaccia, NUC/RIN/TERMO, via Anguillarese 301, I-00060 Rome, Italy
[2]C.E.A. CEC Saclay, IRDI/DEMT/SMTS, F-91191 Gif-sur-Yvette Cedex, France

Abstract

The report describes the experimental results of dynamic tests on reinforced concrete slabs subjected to rigid missile impacts and the comparison between numerical results obtained by finite elements analyses. Two different models have been used in calculation: an homogeneous global model with shell elements and a 3D local model in which concrete and reinforcing bars are really two different coupled material working together with specific constitutive laws.

1. Introduction

In the field of safety for industrial and, especially, for nuclear plants it is necessary to know the structural behaviour of reinforced concrete slabs under dynamic loading by rigid missile impact. In CEA C.E.N. Saclay a series of dynamic tests was performed. The main goals were to investigate the mechanism of the perforation damage and to validate numerical models developed to analyse reinforced concrete structures. In this report the experimental results are compared to those obtained by a global model (SAMSON) and a 3D local model (Drucker-Prager) both implemented in PLEXUS Finite Element code of the CASTEM System.

2. Experimental facility and tests description

Slabs are placed in a horizontal position on four supports located just in the middle of each side. In the center of each slab a steel disk is screwed. A 135 Kg missile drops from a variable height on the steel disk. The slabs geometry and the displacements and forces transducers location are shown in Figg. 1,2. The six displacements transducers, marked from D2 to D7 are MGT-33TA type. To measure the reaction forces on each support is placed a strain gage and SEDEME 75 205 amplifier. An electric contact feeded by direct voltage is placed in the center of the steel disk. The voltage variation gives the time-zero instant for all the measurement points. Along the missile trajectory five optical barriers obtained by means of laser-photodiode couples are placed. The measurement of the heights of these barriers with respect to the impact point and the passing instant of the missile give, by means of the least squares method and

by extrapolation, the missile impact speed. Four slabs for each kind of reinforcing bars are tested:

6 mm diameter reinforcing bars		
Slab N.	Missile Speed (m/s)	Perforation
21	6.48	no
23	8.00	yes
24	7.22	yes
26	6.80	yes

8 mm diameter reinforcing bars		
Slab N.	Missile Speed (m/s)	Perforation
27	5.69	no
28	6.95	yes
29	6.36	yes
30	6.08	yes

Only the slabs N.21, N.26, N.27 and N.30 have been numerically analyzed.

3. Mechanical properties of concrete and steel

For each slab the concrete mechanical properties are here resumed:

Slab N.	Young Modulus (MPa)	Tensile Strenght (MPa)	Compressive Strength (MPa)
21	39850	4.74	48.2
26	39600	3.49	47.7
27	41600	4.51	48.2
30	42500	4.37	41.1

The average values of the main mechanical parameters of the reinforcing bars are listed in the table:

Bars Diameter (mm)	Young Modulus (MPa)	Yield Stress (MPa)	Poisson Ratio
6	241000	483	0.3
8	209000	645	0.3

4. Numeric analyses

Due to the symmetry of the problem, only one-eight of the slab has been studied. In Fig. 3 the mesh made by GIBI pre-processor for the global shell analyses is shown. For the 3D analysis, to represent properly the reinforcing bars, one-fourth of the slab has been taken into account (Figg. 4,5).

SAMSON model

SAMSON is a CASTEM F.E. system program able to give an homogeneous material equivalent, in term of deformations, to the reinforced concret. It is necessary to give the cross section, type and location of the reinforcing bars, stress-strain curve of steel and concrete. We obtain, by SAMSON, the stress-strain curve of an equivalent homogeneous material which has the same moment-bending law than the real material. For each slab calculations have been performed with the real stress-strain curve obtained by SAMSON and three other coarse curves (see, for instance, Fig. 6 for the N.26 slab). The four slabs N.21, N.26, N.27, N.30 have been analysed with this model.

Drucker-Prager model

This model is an extension of the Coulomb model to three-dimensional stress-strain states and it is adequate enough to represent materials which have a poor tensile strenght and a prevalent shear stress failure. The model implemented in PLEXUS code is a simple straight line in the deviatoric-hydrostatic stress space: $\sigma^* = -\beta p + c$

Only the N.21 slab has been analysed by this model with two different elements types (CUBE and CUB8).

5. Calculation results and experimental recordings comparison

For the N.21 (6 mm bars) and N. 30 (8 mm bars) slabs we show in Figg.7,8

the comparison between the measured and calculated displacements by means of SAMSON model in D3/D4 points. Curves N.1, N.3, N.4, give similar results but the N.2 curve, in which a medium elastic modulus has been taken, describes a little different one. In Figg. 9,10 for the same slabs it is compared the impulse on the supports. Reaction forces recordings have been numerically integrated to obtain impulses. In fact supports are unilateral contacts and it is easier for this boundary condition to compare impulses instead of reaction forces. For the N.21 slab in Figg. 11,12 there are the comparison between experimental, shell and 3D calculation for two different measurement points. We can see other interesting mechanical results throught the tickness of the slab. We have to remember that there are two different failure modes: shearing and bending. The maximum shear load arises at the beginning of the transient, at about 0.15 ms. At this instant we can see in Figg. 13,14,15 this effect. Isocourves lie along about 45 degree with respect to the horizontal line and this is the experimental direction of the fractures in perforated slabs. After that, at about 10 ms, slabs reach the maximum bending deflection and the maximum inelastic deformation is in the center (Fig. 16). In the Fig. 17 the zone of the cracked concrete elements is shown.

6. Conclusions

Calculations show that by the two numerical models we obtain results good enough in term of maximum displacement. The transmitted forces on the supports are well evaluated too. There is not much difference between global and local model. This means that SAMSON model is good enough to perform structural analyses in term of deformations. After the maximum deflection, the calculations are not able to follow experimental data maybe because the real punching mechanism is not exactly described in the two models and the bending mode failure is prevalent in the numeric models. Other more accurate models are required to represent this local damage.

7. References

1) Bung. H., Di Giamberardino P., Lepareux M., Matheron Ph. "Rigid missile impact on reinforced concrete slabs. Experimental results and numerical analysis by means of a global model". ENEA Report CT-WHE-00017.(in printing).

2) Bung H., Di Giamberardino P., Lepareux M., "Rigid missile impact on reinforced concrete slabs. Numerical analysis by means of a 3D local model". ENEA Report CT-WHE-00018. (in printing).

3) Bung H., Jamet Ph., Lepareux M., "PLEXUS - Modele de comportament simplifie pour le beton". CEA Report DEMT/SMTM/LAMS/84-095.

4) Chavant C., Lepareux M., "Systeme CEASEMT - Le model de Drucker-Prager pour la rupture du beton dans le programme PLEXUS". CEA Report DEMT/SMTM/LAMS/82-014.

5) Barbe B., Hoffmann A., Jamet P., Lepareux M., Maurel P., Millard A. "Ultimate Flexural Behaviour of Reinforced Concrete Shells Under Static and Dynamic Loading". Paper J 1/8, SMIRT 8; Brussels - August 19-23, 85.

6) Lepareux M., Matheron Ph., Jamet Ph., Lieutenant J.L., Couilleaux J., Lazare-Chopard G., Riviere J. "Ultimate behaviour of reinforced concrete shell under static and dynamic loading". SMIRT 9 Lausanne August 17-21, 87.

7) Matheron Ph., "Sûreté des usines - calcul à la ruine de dalles simples Interaction flexion-perforation (0129-03)"CEA Report DEMT/SMTM/LAMS 88-141.

8) Lieutenant J.L., M. Lepareux. "Programme PLEXUS - Sûreté des Usines - Calcul à la ruine d'une dalle en béton armé avec un modèle massif tridimensionnel"(0129-03). CEA Report DEMT/SMTM/LAMS/88-142.

9) Lieutenant J.L., "Calcul SAMSON - materiau equivalent a une dalle de beton ferraille". CEA Report DEMT/SMTS/LAMS/83-006.

10) Lieutenant J.L., Lepareux M. "PLEXUS 3D - Comportement dynamique elasto-plastique de dalle en beton arme. Dalle 8-9-10" CEA Report DEMT/SMTS/LAMS/83-110.

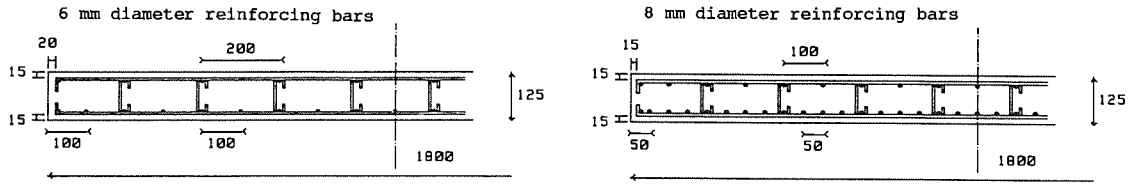

Fig.1 - Geometry and reinforcing bars location.

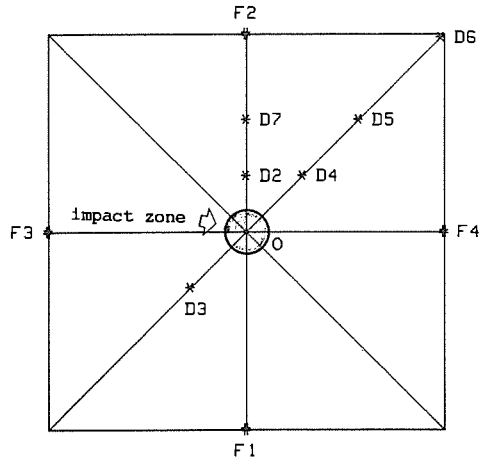

Fig.2 - Displacements and forces transducers location.

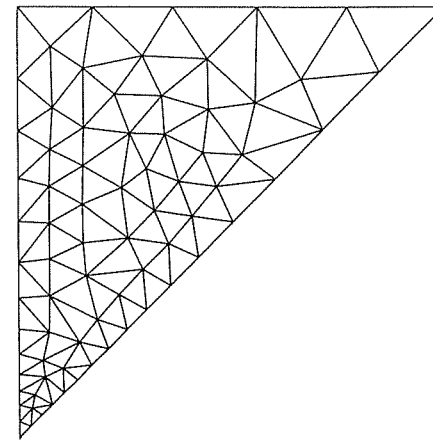

Fig.3 - Shell elements mesh for global analysis.

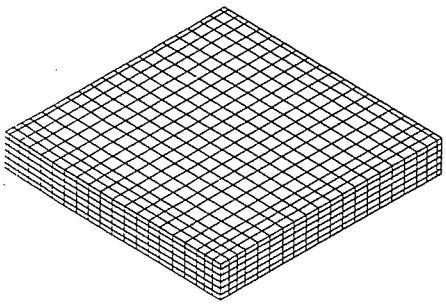

Fig.4 - 3D mesh: concrete

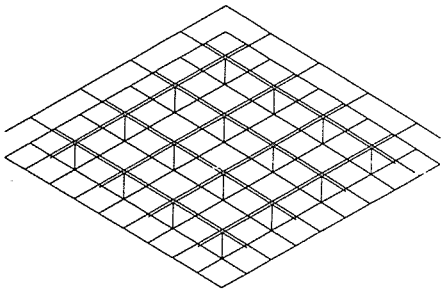

Fig.5 - 3D mesh: reinforcing bars

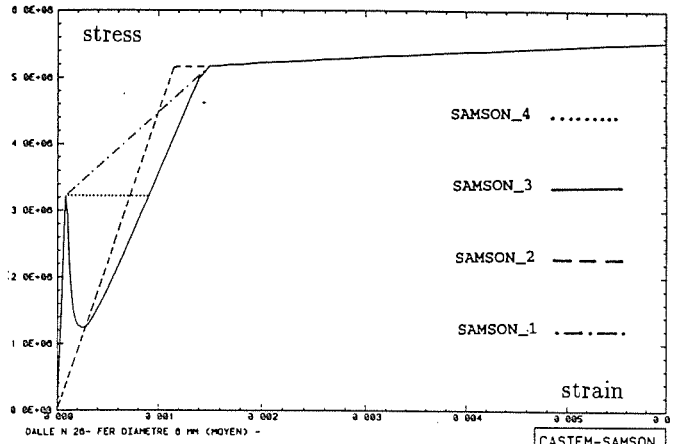

Fig.6 - Equivalent stress-strain curve by SAMSON.

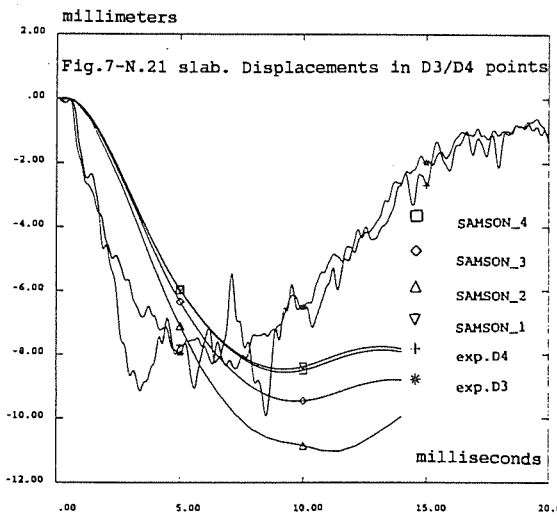

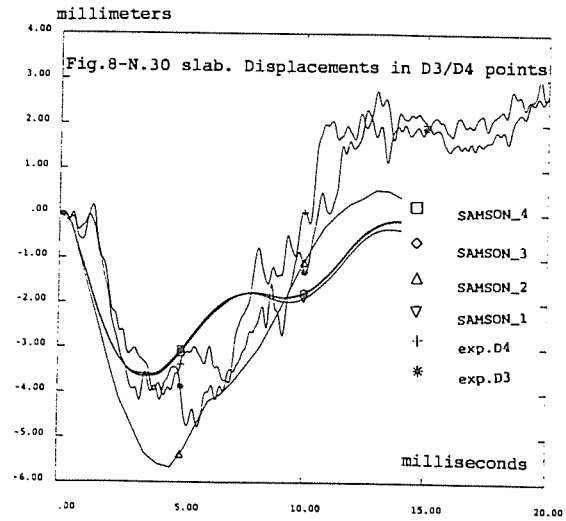

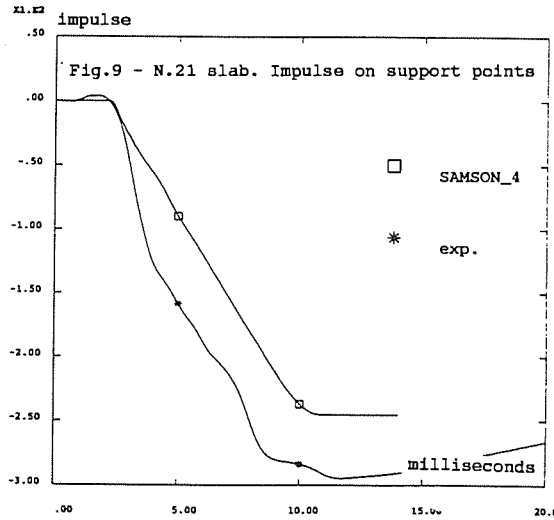

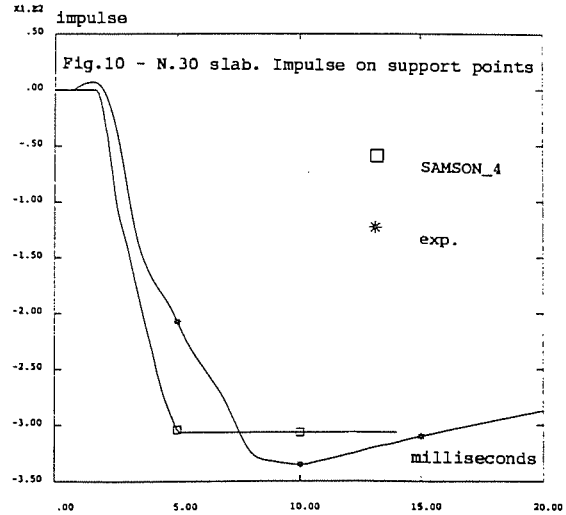

Fig.11 - N.21 slab. Displacements in D3/D4 points.

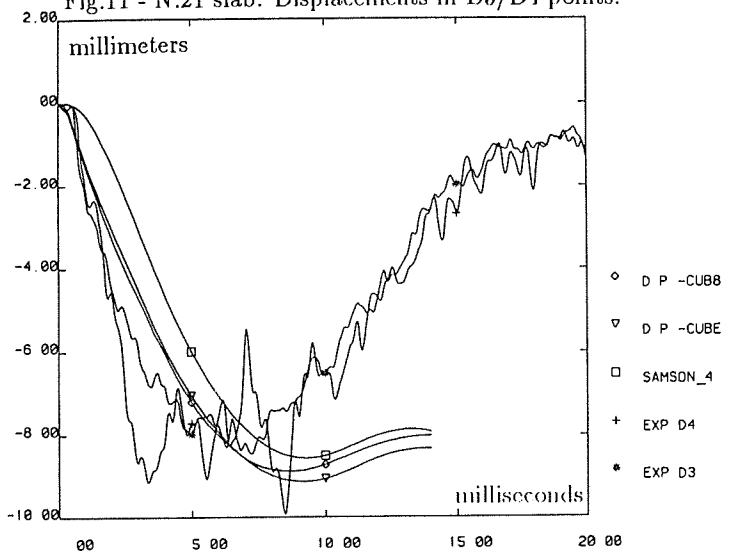

Fig.12 - N.21 slab. Displacements in D7 point.

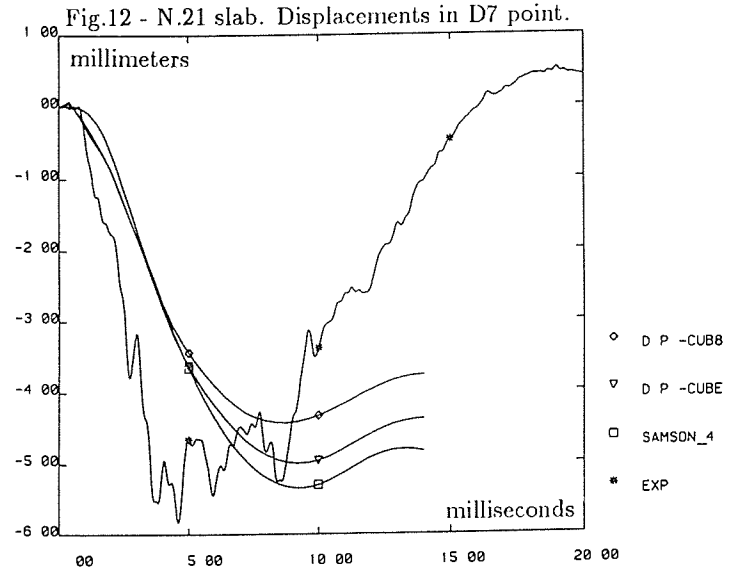

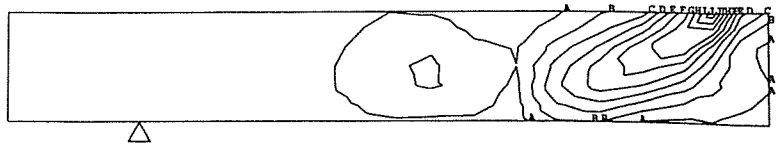

Fig.13 - Maximum punching load: shear stress isocurves.

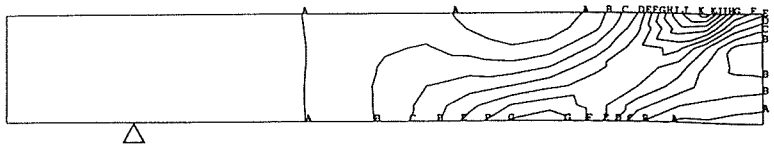

Fig.14 - Maximum punching load: deviatoric stress component.

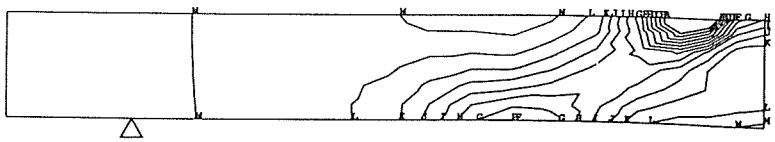

Fig.15 - Maximum punching load: hydrostatic stress component.

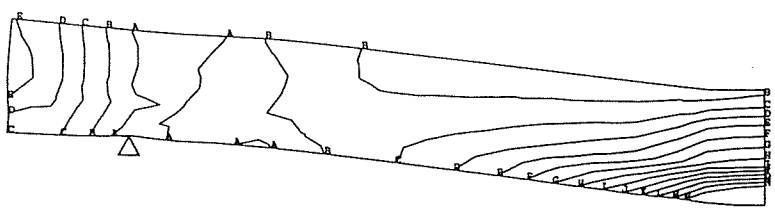

Fig.16 - Maximum bending load: inelastic strain.

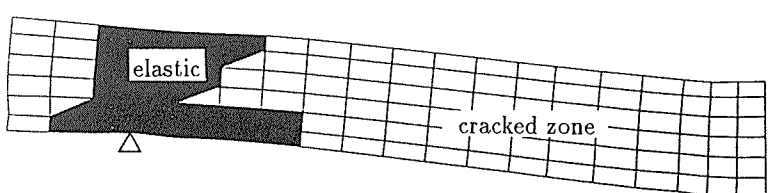

Fig.17 - Maximum extension of cracked zone.